REPORT DOCUMENTATION PAGE

Form Approved OMB No. 0704-0188

1. REPORT DATE *(DD-MM-YYYY)*	2. REPORT TYPE	3. DATES COVERED *(From – To)*
27-11-2007	Final Report	15 November 2006 - 07-Jul-09

4. TITLE AND SUBTITLE

Electronic structure investigations of aluminum clusters

5a. CONTRACT NUMBER
FA8655-07-1-3030

5b. GRANT NUMBER

5c. PROGRAM ELEMENT NUMBER

6. AUTHOR(S)

Professor JOHN P Maier

5d. PROJECT NUMBER

5d. TASK NUMBER

5e. WORK UNIT NUMBER

7. PERFORMING ORGANIZATION NAME(S) AND ADDRESS(ES)
University of Basel
Klingelbergstrasse 80
Basel CH-4056
Switzerland

8. PERFORMING ORGANIZATION REPORT NUMBER

N/A

9. SPONSORING/MONITORING AGENCY NAME(S) AND ADDRESS(ES)

EOARD
Unit 4515 BOX 14
APO AE 09421

10. SPONSOR/MONITOR'S ACRONYM(S)

11. SPONSOR/MONITOR'S REPORT NUMBER(S)
Grant 07-3030

12. DISTRIBUTION/AVAILABILITY STATEMENT

Approved for public release; distribution is unlimited. (approval given by local Public Affairs Office)

13. SUPPLEMENTARY NOTES

14. ABSTRACT

This report results from a contract tasking University of Basel as follows: The Grantee will investigate spectroscopic studies of aluminum clusters and their ions. Various techniques will be used. With the experience using laser-ablation sources the grantee's machines will be adapted to produce aluminum clusters. Previous studies have demonstrated that using the second harmonic of a YAG laser can produce a wealth of aluminum molecules of assorted sizes.1,2 Mass spectra from these ablation experiments have shown that clusters ranging from Al8- to beyond Al18- can be created. It is the goal of this study to employ similar methods to produce and spectroscopically interrogate these species. In one year it is expected that the preliminary spectra for the smaller Al clusters, both neutral and ionic, will be investigated.

15. SUBJECT TERMS
EOARD, high energy density matter, Propellants, aluminium clusters

16. SECURITY CLASSIFICATION OF:			17. LIMITATION OF ABSTRACT	18, NUMBER OF PAGES	19a. NAME OF RESPONSIBLE PERSON
a. REPORT	b. ABSTRACT	c. THIS PAGE			BARRETT A. FLAKE
UNCLAS	UNCLAS	UNCLAS	UL	23	**19b. TELEPHONE NUMBER** *(Include area code)* +44 (0)1895 616144

Final Deliverable: Grant FA8655-07-3030

This is the final report for the EOARD project "Electronic structure investigations of aluminium clusters". A one year grant commenced 15. November 2006 and terminated 14. November 2007. An interim report for the first 6 months was sent in and approved.

We proposed to study the electronic spectra of aluminium containing molecules and for this purpose a number of the techniques developed/used by us in Basel were made available for such measurements. In the year of the project we used two techniques, resonance two-color two-photon ionization (R2C2PI) spectroscopy and laser induced fluorescence (LIF) to probe the aluminium containing species produced within a supersonic pulsed expansion incorporating either laser vaporation of aluminium or a discharge source. With the R2C2PI set up we could identify by mass-spectrometry the production of the bare aluminium clusters, Al_n. The addition of acetylene into the laser vaporization region produced, among other species, AlCCH, and we managed to observe and assign the electronic spectrum of this molecule for the first time. The rotational structure could be resolved and the analysis of this pattern, backed up by ab initio calculations, proved that it is the linear isomer AlCCH which was observed. An article reporting the results has been published in Physical Chemistry and Chemical Physics:

"Gas phase electronic spectrum of linear AlCCH"
C.Apetrei, H.Ding and J.P.Maier,
Physical Chemistry Chemical Physics, 9, 3793, 2007, (copy as attachment).
The article and this research was highlighted by using it for the front cover of the journal (copy as attachment).
Cristina Apetrei (PhD student) and a research associate Dr.H.Ding carried out these studies in Basel.

Using the LIF approach, with a same source as that produced AlCCH, we observed an electronic transition of cyclic AlC_2. This is proven by rotational analysis of the structure seen in the spectrum, predictions given by ab initio calculations, carried out in collaboration with Dr.Isabelle Navizet, a member of the theoretical group at the University of Marnee la Vallee, France, and by observing this transition with the R2C2PI technique. An article presenting these results has been published:

"Electronic spectrum of the AlC_2 radical"
E.Chasovskikh, E.Jochnowitz, E.Kim and J.P.Maier
J.Physical Chemistry A, 111, 11986, 2007, (copy as attachment).

E.Chasovskikh (PhD student) and two postdocs in the group, Dr.E.Jochnowitz and Dr.Eunsoon Kim were involved in these investigations.

Thus the year's project has been successful: laser ablation and discharge sources have been put into operation for the production of aluminium clusters, the electronic spectra of two new species, linear AlCCH and cyclic AlC_2 have been observed for the first time and two articles published on this in leading journals of chemical physics. The two publications acknowledge the sponsorship by EOARD, as will the third manuscript, still in preparation.

During the ıre of this EOARD project, in collabo ɔn with Prof. Alan Knight, Griffith University, Brisbane, Australia, who spent his sabbatical leave with us in 2007, a laser vaporization source incorporating two rotating rods was built. In the last months of the project we could demonstrate that this is a viable approach; using an aluminium and carbon rod the observed spectrum of AlC_2 could be readily obtained. This opens up the possibility of producing a number of mixed aluminium clusters.

J.P.Maier attended the annual "Molecular Dynamics Contractors Meeting", 20-22 May, Irvine, California, U.S.A., on the invitation of Dr.M.Berman, and presented the results on the new linear AlCCH and cyclic AlC_2 species in a poster.

Disclaimer: The view and conclusions contained in the publications arising as result of the sponsorship by EOARD, are those of the author and should not be interpreted as necessarily representing representing the official policies or endorsements, either expressed or implied, of the Air Force Office of Scientific Research or the U.S. Government.

Disclosure of inventions: "I certify that there were no subject inventions to declare during the performance of this grant".

J. P. Maier

Professor John P.Maier

PCCP

Physical Chemistry Chemical Physics

An international journal

www.rsc.org/pccp

Volume 9 | Number 29 | 7 August 2007 | Pages 3793–3924

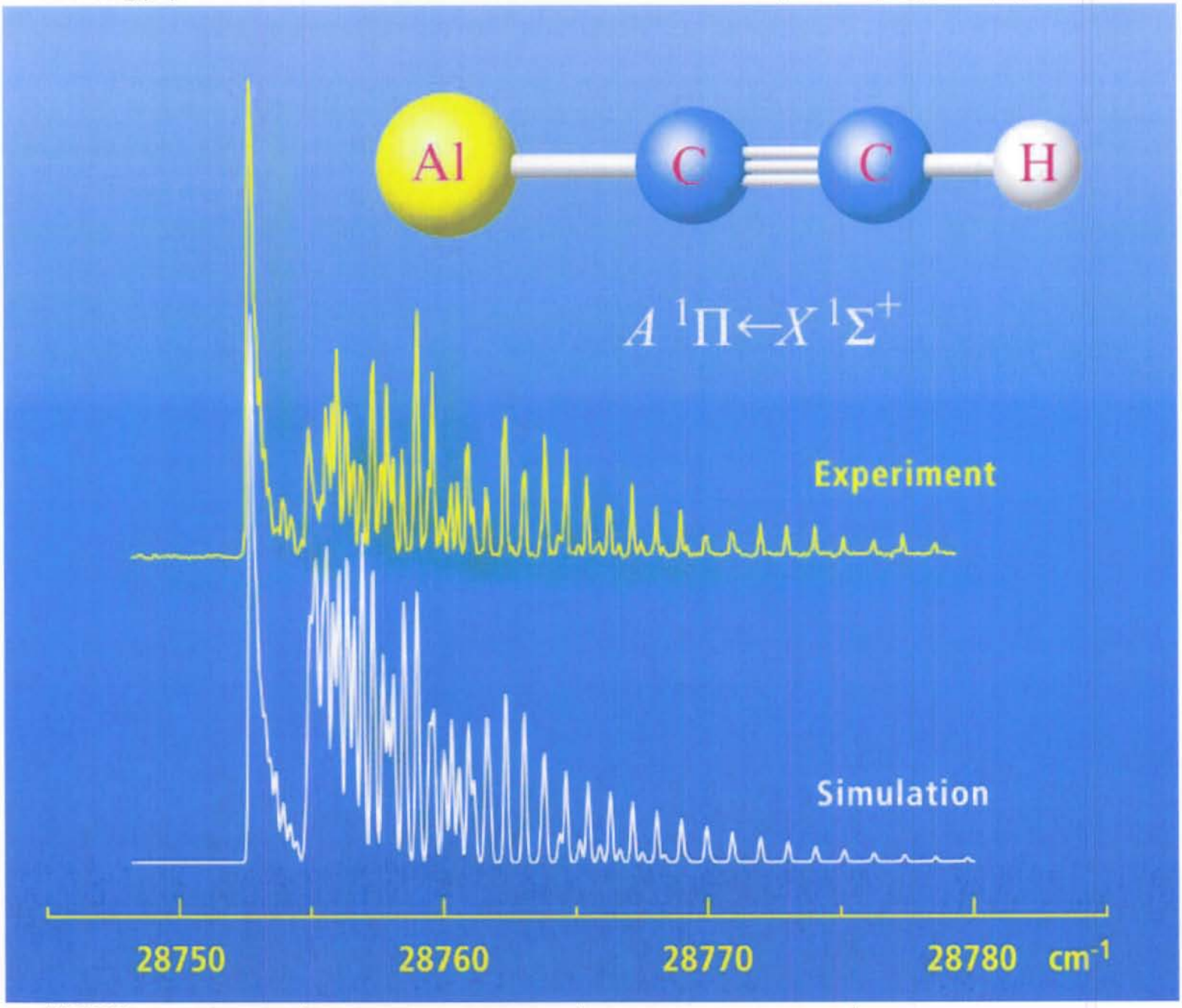

ISSN 1463-9076

COVER ARTICLE
Maier *et al.*
Gas phase electronic spectrum of linear AlCCH

HOT ARTICLE
Johansson *et al.*
Extended Förster theory for determining intraprotein distances: an accurate analysis of fluorescence depolarisation experiments

1463-9076(2007)9:29;1-C

Gas phase electronic spectrum of linear AlCCH

Cristina Apetrei, Hongbin Ding and John P. Maier*

Received 27th April 2007, Accepted 21st May 2007
First published as an Advance Article on the web 14th June 2007
DOI: 10.1039/b706384a

The electronic spectrum of the aluminium containing species AlCCH has been detected in the gas phase in the region 315–355 nm. The experiment used a mass selective resonant two-color two-photon ionization technique coupled to a laser ablation source. Structures of the AlCCH isomers have been optimized using density functional theory (DFT) and the excitation energies to the low-lying electronic excited states calculated. Based on the analysis of the observed rotational structure and the theoretical data, the spectrum is assigned to the $A\,^1\Pi \leftarrow X\,^1\Sigma^+$ electronic transition of linear AlCCH. The vibronic band system is complicated by the Renner–Teller effect in the excited state. The assignment yields $\nu_4'' = 516.4\ cm^{-1}$ for the stretching mode in the ground $X\,^1\Sigma^+$ state and $\nu_4' = 654.5\ cm^{-1}$ for $A\,^1\Pi$ excited state. Molecular constants determined from the rotational analysis are $B_0'' = 0.16487(14)$, $B_0' = 0.17845(13)$ and $T_0 = 28\,755.04\ cm^{-1}$. The experimental and theoretical data indicate a shorter Al–C bond in the $A\,^1\Pi$ excited than the $X\,^1\Sigma^+$ ground state.

1. Introduction

Over the past thirty years of radio astronomy, a great deal has been learned about interstellar molecules and their chemistry. Despite this progress, there are still areas of molecular astrophysics where challenges remain. One of these concerns the chemistry and distribution of molecules containing metals. Identifying the carriers of these elements in the interstellar medium, including circumstellar gas, is crucial for the evaluation of dust grain composition, ionization balance, mass loss and elemental depletions from evolved stars.

To date, nine molecules containing the metals aluminium, magnesium, sodium, and potassium have been discovered toward circumstellar envelopes of carbon-rich stars such as IRC + 10216 and CRL 2688.[1] These species fall into two classes: the cyanides MgNC,[2] MgCN,[3] NaCN,[4] KCN, and AlNC[5] and the halide compounds AlCl, AlF, KCl, and NaCl.[6,7] It seems that the most common metallic element in IRC + 10216 is aluminium.[8] At the same time stable species such as CO, C_2H_2 and HCN have been detected in this carbon-rich object.[9,10] It was postulated that these molecules photodissociate in the star's outershell resulting in the formation of C_2H, C_4H and C_6H radicals.[11] The products could react with Al atoms to form AlCCH, a molecule with potential interest in astrophysics.

However, how metal species bond to hydrocarbon species has not been extensively explored, at least from a spectroscopic point of view. Reaction products of metal atoms and hydrocarbon molecules are important for understanding chemisorption and catalytic processes. A number of metal atom reactions with acetylene have already been studied.[12–15] Aluminium adducts with acetylene have been examined using *ab initio* calculations, and a number of stable Al–C_2H_2 isomers have been predicted.[16–18] The related reaction between laser ablated Al atoms and acetylene has been examined using IR matrix isolation spectroscopy.[19] It was found that Al atom and C_2H_2 form the AlC_2H_2 complex. This relaxes in the matrix to form HAlCCH and under photolysis produces the AlCCH molecule.

Several gas phase studies of the electronic spectra of metal–ligand radicals such as MgCCH, CaCCH and SrCCH have been reported.[20–22] All three radicals exhibit an $A\,^2\Pi \leftarrow X\,^2\Sigma^+$ electronic transition in the visible spectral range and it could be concluded that replacing a H atom with a metal atom results in a linear metal–acetylide species.

In this article the electronic spectrum of AlCCH is presented and analyzed for the first time. The experimental technique used two-color two-photon laser ionization in a supersonic molecular beam.

2. Experiment

The experimental instrument consists of a molecular beam combined with a mass spectrometer.[23] The beam was produced by laser ablation of an aluminium rod in the throat of a pulsed supersonic expansion of 1% acetylene in helium or neon at a backing pressure of ~10 bar using a pulsed Nd:YAG laser for ablation (532 nm, 30 mJ $pulse^{-1}$). The carrier gas and products of ablation flowed through a 15 mm long, 3 mm diameter channel, which then expands into a vacuum chamber. This was skimmed to form a collimated beam of neutral and ionized molecules. Ions were then removed by a perpendicular electric field before entering the ionization region of a Wiley–McLaren time-of-flight mass spectrometer,[24] where the molecules were irradiated with a pulse of tunable ultraviolet-visible radiation. Following a short delay the molecules were exposed to a pulse of 193 nm photons from an ArF excimer laser. The combination of the UV and the 193 nm photons was sufficient to ionize AlCCH.

Department of Chemistry, University of Basel, Klingelbergstrasse 80, CH-4056 Basel, Switzerland. E-mail: j.p.maier@unibas.ch; Fax: +41-61-267-38-55

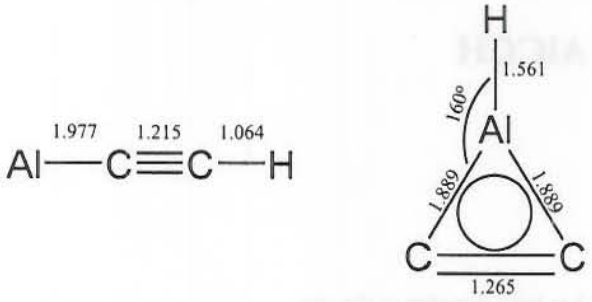

Fig. 1 Calculated ground state structures of AlCCH using DFT-B3LYP/aug-cc-pvtz level of theory (bond-lengths in Å).

The signal from the microchannel plate ion-detector was sent to a fast oscilloscope followed by data acquisition.

The resonant two-color two-photon (R2C2PI) spectrum of AlCCH was investigated over the 300–700 nm range. Excitation photons were provided from an OPO system ($\sim$5 cm^{-1} band-width) for the vibronic survey scans. A pulsed dye laser was used ($\sim$0.1 cm^{-1}, $\sim$5 mJ pulse^{-1}) for the rotationally resolved work. Calibration was accomplished using a wavemeter for the vibronically resolved work. The dye laser was calibrated with optogalvanic spectra obtained from a Fe/Ne hollow cathode lamp.

3. Theoretical calculations

Ab initio calculations were carried out with the GAUSSIAN 98 suite of programs.[25] Geometry optimizations and energy calculations for two isomers (Fig. 1) have been performed at the B3LYP/aug-cc-pvtz level of theory. The calculated harmonic vibrational frequencies, rotational constants and dipole moments in the ground states of linear-AlCCH and cyclic-HAlCC are listed in Tables 1 and 2. The results are in agreement with those obtained with the CASSCF method.[19] These show that the linear structure is more stable than the cyclic one by 41.1 kJ mol^{-1}. Calculations for other isomers, such as HAlCC, bent-AlCCH, have been carried out and indicate that HAlCC is unstable and converges to cyclic-HAlCC, while bent-AlCCH leads to the linear-AlCCH.

The electronic configuration of the ground state linear-AlCCH is $\ldots[8\sigma]^2[3\pi]^4[4\pi]^4[9\sigma]^2$, $X\,^1\Sigma^+$ and $\ldots[3b_2]^2[2b_1]^2[7a_1]^2[8a_1]^2$, $X\,^1A_1$ for the cyclic-HAlCC. *Ab initio* calculations of the excited states were undertaken using time-dependent density functional theory.[26] The ground state of linear-AlCCH is dominated by the $\ldots4\pi^4 9\sigma^2$ electronic configuration. Promotion of the electron from $9\sigma \rightarrow 5\pi$ leads to the $\ldots[8\sigma]^2[3\pi]^4[4\pi]^4[9\sigma]^1[5\pi]^1$ configuration, resulting in the $A\,^1\Pi$ first electronic excited state. The $8a_1 \rightarrow 4b_2$ excitation for the cyclic-HAlCC leads to the $\ldots[3b_2]^2[2b_1]^2[7a_1]^2[8a_1]^1[4b_2]^1$ configuration, resulting in the $A\,^1B_2$ excited state. The calculated vertical electronic excitation energies and oscillator strengths (f) for the linear and cyclic isomers are listed in Table 3.

Table 1 *Ab initio* calculated harmonic vibrational frequencies (cm^{-1}) for linear and cyclic isomers in their ground states at the DFT-B3LYP/aug-cc-pvtz level

Frequencies	AlCCH ($C_{\infty v}$)	HAlCC (C_{2v})
ν_1	3438 (σ)	2028 (a_1)
ν_2	2065 (σ)	1807 (a_1)
ν_3	733 (π)	754 (a_1)
ν_4	503 (σ)	522 (b_2)
ν_5	132 (π)	459 (b_1)
ν_6		415 (b_2)

Table 2 Calculated energies, rotational constants and dipole moments in the ground state of linear and cyclic isomers at the DFT-B3LYP/aug-cc-pvtz level

	AlCCH ($C_{\infty v}$)	HAlCC (C_{2v})
A/cm^{-1}		1.5571
B/cm^{-1}	0.16385	0.3668
C/cm^{-1}		0.3034
D_e/Debye	0.549[a]	4.530[a]
E/a.u.	−319.216	−319.153
ΔE/eV	0.0	1.71

[a] Dipole moment along the C_∞ and C_2 axis, respectively.

4. Results and discussion

4.1 Electronic spectrum and the carrier

Fig. 2 displays the electronic spectra of AlCCH (m/z = 52) and its isotopomer (m/z = 53) obtained by laser ablation of an Al rod in the presence of 1% C_2H_2 in a He gas mixture. The maxima of the vibronic bands are listed in Table 4.

The overall appearance of the origin band, measured at 0.1 cm^{-1} resolution, shows the general PQR pattern expected for a linear $^1\Pi \leftarrow X\,^1\Sigma^+$ transition. *Ab initio* calculations predict that linear-AlCCH with $C_{\infty v}$ symmetry is the most stable isomer. The second isomer (cyclic-HAlCC) is a local minimum located $\sim$1.71 eV higher in energy. Based on this energy difference it could be expected that linear-AlCCH will be the major contributor to the observed spectrum in a supersonic molecular beam. The TD-DFT calculations predict that the vertical transition energy of the $A\,^1\Pi \leftarrow X\,^1\Sigma^+$ system of linear-AlCCH is 3.64 eV (Table 3). This is in good agreement with the observed transition energy (3.57 eV) of the origin band. The transition energy for the cyclic isomer is also in the range of the experimental spectrum but is likely to have a minor contribution due to its weak oscillator strength

Table 3 Vertical transition energies and oscillator strengths (f) for linear and cyclic isomers at the optimized ground state geometries calculated using TD-DFT with aug-cc-pvtz basis sets

	AlCCH ($C_{\infty v}$)		HAlCC (C_{2v})		Experiment
State	T_0/eV	f	T_0/eV	f	T_0/eV
X	0.00 ($^1\Sigma^+$)		0.00 ($^1A_1$)		
1	3.64 ($^1\Pi$)	9.9×10^{-2}	3.83 ($^1B_2$)	1.6×10^{-3}	3.57
2	4.70 ($^1\Sigma^-$)	0	4.04 ($^1B_1$)	1.1×10^{-3}	
3	4.77 ($^1\Delta$)	0	4.58 ($^1A_2$)	0	
4	5.62 ($^1\Sigma^+$)	4.1×10^{-2}	4.81 ($^1A_1$)	7.6×10^{-3}	
5	5.78 ($^1\Sigma^+$)	1.5×10^{-1}	5.57 ($^1A_1$)	3.1×10^{-2}	
6	5.85 ($^1\Pi$)	6.8×10^{-2}	5.84 ($^1B_1$)	3.2×10^{-2}	
7	5.87 ($^1\Sigma^+$)	2.1×10^{-1}	6.01 ($^1B_2$)	5.6×10^{-3}	
8	6.25 ($^1\Sigma^+$)	1.1×10^{-1}	6.17 ($^1A_2$)	0	
9	6.84 ($^1\Pi$)	5.1×10^{-2}	6.22 ($^1B_2$)	5.6×10^{-2}	

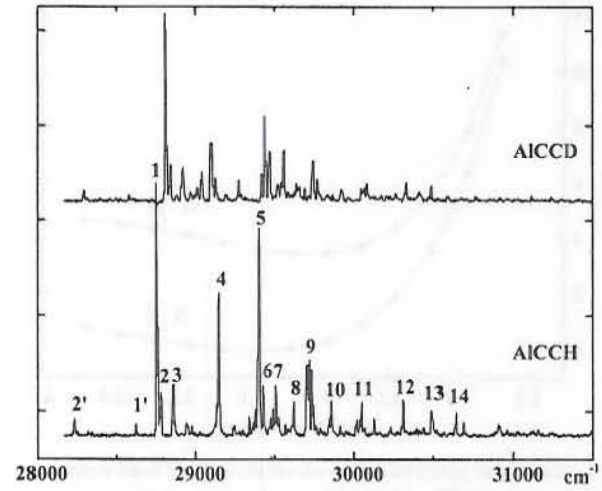

Fig. 2 Observed $A\,^1\Pi \leftarrow X\,^1\Sigma^+$ electronic spectra of AlCCH and AlCCD measured by a resonant two-color two-photon ionization technique in a supersonic molecular beam.

(Table 3). Other predicted high lying transitions for both the linear and cyclic isomers were beyond the range of the probe laser.

4.2 Vibronic bands of AlCCH

The observed spectrum is assigned as the $A\,^1\Pi \leftarrow X\,^1\Sigma^+$ electronic transition of linear AlCCH. The vibronic bands reveal a complicated structure (Fig. 2). Band 1 is assigned as the origin transition because it is the first strong peak in the low energy region and is not sensitive to the experimental conditions (temperature). The determined T_0 of the origin band is 3.57 eV, which is in good agreement with the calculated value (3.64 eV). Band 2′, located 516.4 cm^{-1} to the red of the origin is assigned as the 4_1^0 transition, the ν_4'' Al–C stretching motion in the ground state. This value is in accord with the calculated (503 cm^{-1}) and matrix (512.8 cm^{-1}) data.[19] Upon deuteration, the band hardly shifts (516.4 cm^{-1} to 513.6 cm^{-1}), indicating that the vibrational motion involves only the Al and C atoms.

Table 4 Vibronic bands in the $A\,^1\Pi \leftarrow X\,^1\Sigma^+$ system of AlCCH and AlCCD

	ν/cm^{-1}		$\Delta\nu$/cm^{-1}		
Label	AlCCH	AlCCD	AlCCH	AlCCD	Assignment
2′	28 233.3	28 293.3	−516.4	−513.6	4_1^0 (Al–C stretch)
1′	28 624.8	28 577.1	−126.0	−229.7	Hot band
1	28 749.7	28 806.9	0	0	0_0^0 ($A\,^1\Pi \leftarrow X\,^1\Sigma^+$)
2	28 784.1	28 843.3	34.4	36.4	ν_5' (AlCC bend)
3	28 864.3	28 921.9	114.5	115	ν_5' (AlCC bend)
4	29 149.6	29 103.7	399.9	29 6.9	ν_3' (CCH bend)
5	29 404.2	29 435.4	654.5	628.5	4_0^1 (Al–C stretch)
6	29 427.0	29 468.1	677.3	661.2	(AlCC bend)
7	29 505.7	29 563.3	756.0	756.5	(AlCC bend)
8	29 623.8	29 635.9	874.0	829.1	(AlCC bend)
9	29 721.5	29 740.1	971.8	933.2	(AlCC bend)
10	29 857.3	29 921.7	1107.6	1114.8	(AlCC bend)
11	30 051.2	30 081.0	1301.5	1274.1	4_0^2 (Al–C stretch)
12	30 310.8	30 332.9	1561.1	1526.0	
13	30 485.5	30 491.1	1735.8	1684.2	
14	30 640.0		1890.0		

Band 2 is located 34.4 cm^{-1} to the blue of the origin. Theoretical calculations predict that the lowest vibrational frequency ν_5'', is about 130 cm^{-1}, which is much larger than 34.4 cm^{-1}. However, in the degenerate $A\,^1\Pi$ state, the ν_5' vibrational mode of π-symmetry is subject to a Renner–Teller effect. This causes vibrational levels with $v_5' \neq 0$ to split into components. There are two vibrational modes ν_3' and ν_5' with π-symmetry for linear AlCCH. The observed vibronic pattern indicates that both ν_3' and ν_5' are involved in the Renner–Teller interaction. Bands 2 and 3 can be assigned as the transitions arising from components of ν_5', supported by the small shift upon deuteration. Band 4 shows a large isotopic change and thus is assigned as a component of the CCH bending mode ν_3'. The calculations give the vibrational frequency of the Al–C stretch mode as 600 cm^{-1} in the $A\,^1\Pi$ state, leading to the attribution of bands 5 and 11 as the 4_0^1 and 4_0^2 transitions. A clear designation for individual bands is difficult because of the Renner–Teller effect on ν_3' and ν_5' modes. The suggested vibronic assignments are given in Table 4.

4.3 Rotational structure

The origin band of the $A\,^1\Pi \leftarrow X\,^1\Sigma^+$ transition that was rotationally resolved with a modest resolution of 0.1 cm^{-1}, along with the simulation of the spectrum based on the least squares fit of the lines are shown in Fig. 3. To obtain a fit, the Σ^+ and Π symmetries in the X and A states as predicted by *ab initio* calculations for the linear isomer were used.

The calculated ground state rotational constant (Table 2) was used as a reasonable starting point in the simulation. The P-branch band-head shows that the rotational constant in the excited state is larger. The simulation[27] was performed by systematically adjusting the rotational constant in the $A\,^1\Pi$ state, while varying the spectroscopic line-width from 0.1 cm^{-1} to 0.2 cm^{-1} and rotational temperatures from 25 to 50 K. Good agreement between the experiment and simulation was achieved using 0.16 cm^{-1} and 45 K. Variations in line

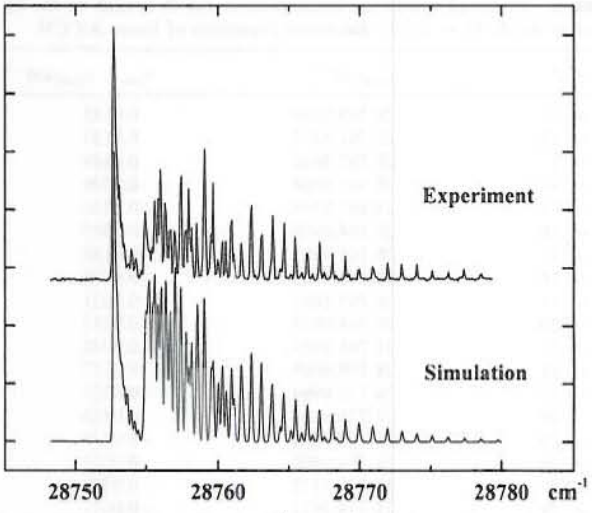

Fig. 3 The origin band in the $A\,^1\Pi \leftarrow X\,^1\Sigma^+$ electronic transition for the AlCCH. The rotational temperature employed in the simulation is 45 K.

Table 5 Molecular parameters determined from the least square fit of the spectrum for AlCCH

Parameter	$X\,^1\Sigma^+$	$A\,^1\Pi$
T_0/cm^{-1}	0	28 755.0455(50)[a]
B_0/cm^{-1}	0.16487(14)[a]	0.17845(13)[a]
$r_{Al-C}/Å$	1.96830	1.85235

[a] Values in parentheses denote one standard deviation and apply to the last digits of the constants.

intensities between the experimental and simulated spectra are mainly due to the ablation source instability.

Rotational line assignments were made by comparing the observed spectral lines with the calculated ones. The linear least square fit was performed using forty rotational lines and floating the rotational constants for ground and excited state. The derived spectroscopic constants are given in Table 5. Higher order terms, such as centrifugal distortion or lambda-doubling parameter, q, were not included in the model as the spectral resolution used was inadequate.

Table 6 lists the frequencies recorded for 20 separate rotational transitions of linear AlCCH. The lines are assigned as part of the R-branch. The analysis indicates that while this branch partially overlaps with Q- and P-ones, the assignment of the R-lines was possible because their intensity is higher. Individual overlapping lines from the Q-branch can not be easily distinguished due to high density of spectral lines. The shape of the P-branch is of a band head, thus making individual line assignment difficult. The T_0 line calculated from the simulations is at 28 755.04 cm^{-1}.

The derived rotational constant analysis shows that the Al–C bond-length decreases significantly in the $A\,^1\Pi$ electronic excited state (Table 5). This indicates that Al–C is more bonding in the excited than in the ground state. The potential energy curves along the Al–C bond stretching coordinate for the ground and the excited states have been calculated for a better understanding of the bonding changes (Fig. 4). These

Table 6 Observed rotational frequencies in the R-branch of the 0_0^0 band in the $A\,^1\Pi \leftarrow X\,^1\Sigma^+$ electronic transition of linear AlCCH

$J' \rightarrow J''$	ν_{obs}/cm^{-1}	$\nu_{obs} - \nu_{calc}/cm^{-1}$
12 → 11	28 760.9509	0.0155
13 → 12	28 761.6339	0.0153
14 → 13	28 762.3640	0.0349
15 → 14	28 763.0964	0.0296
16 → 15	28 763.8568	0.0250
17 → 16	28 764.6909	0.0669
18 → 17	28 765.4266	−0.0168
19 → 18	28 766.2723	−0.0178
20 → 19	28 767.1661	0.0021
21 → 20	28 768.0839	0.0187
22 → 21	28 768.9984	0.0048
23 → 22	28 769.9609	0.0177
24 → 23	28 770.8994	−0.0327
25 → 24	28 771.9548	0.0126
26 → 25	28 772.9620	−0.0176
27 → 26	28 774.0380	−0.0062
28 → 27	28 775.1175	−0.0188
29 → 28	28 776.2622	−0.0071
30 → 29	28 777.3382	−0.0632
31 → 30	28 778.5758	0.0008

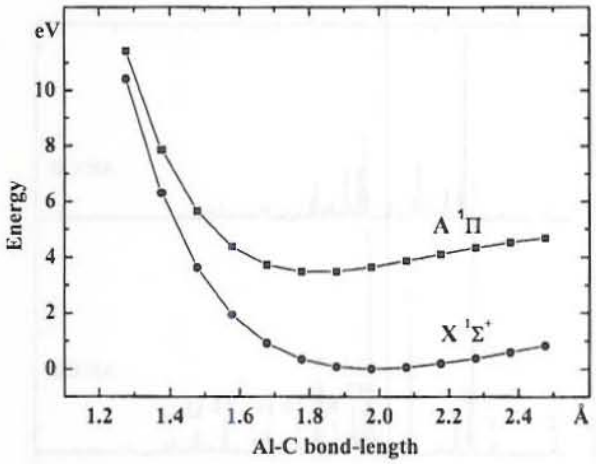

Fig. 4 Calculated potential energy curves along Al–C bond stretching coordinate using DFT method with aug-cc-pvtz basis sets.

give an Al–C bond-length as 1.977 Å in the $X\,^1\Sigma^+$ and 1.775 Å in the $A\,^1\Pi$ state, a ~10% decrease. The constants inferred from the rotational analysis yield a decrease of ~6%. The calculations indicate that the highest occupied molecular orbital (HOMO), 9σ, is 78% dominated by the 3s orbital of Al atom, antibonding in nature, whilst the lowest unoccupied molecular orbital (LUMO), 5π, is largely (92%) the $3p_x3p_y$ atomic orbital of Al with bonding character. The transition of the electron from the HOMO to LUMO leads to a decrease in the Al–C bond-length. This effect has also been observed in the isoelectronic molecule AlCN,[28] as well as in other metal mono-acetylides, such as MgCCH,[20] CaCCH[21] and SrCCH.[22]

5. Conclusions

An electronic spectrum of linear AlCCH has been obtained using a resonant two-color two-photon ionization technique. The complicated vibronic structure in the $A\,^1\Pi \leftarrow X\,^1\Sigma^+$ band system is due to a Renner–Teller effect involving the two vibrational modes, ν_3' and ν_5'. An analysis yields $\nu_4'' = 516.4\ cm^{-1}$ for the stretching mode in the ground state and $\nu_4' = 654.5\ cm^{-1}$ in the $A\,^1\Pi$ state.

The rotational structure apparent for the origin band shows that AlCCH is linear both in its ground $X\,^1\Sigma^+$ and first excited $A\,^1\Pi$ electronic state, the latter being characterized by a decrease in the Al–C bond-length, a behavior similar to other metal mono-acetylides.

Regarding the astrophysical interest it is difficult to compare the observed AlCCH electronic transitions with the diffuse interstellar bands data because there are few discrete absorptions below ~400 nm.[29] However, AlCCH is likely to be present in carbon-rich stars where the isoelectronic molecule AlNC as well as other aluminium-bearing compounds have been detected, in particular in IRC + 10216 and CRL 2688.[5,6] Although AlCCH is closed-shell, it probably lacks the stability of more robust species such as AlF and AlCl detected in the dense inner envelope of these stars. Thus one would expect to find aluminium acetylide toward the outer-shell. The rotational constants deduced here also may provide the basis for

the search of the millimeter-wave spectrum of AlCCH in the laboratory.

Acknowledgements

This work has been supported by the Swiss National Science Foundation (Project No. 200020-115864/1) and the European Office of Aerospace Research and Development.

References

1 J. L. Highberger, K. J. Thomson, P. A. Young, D. Arnett and L. M. Ziurys, *Astrophys. J.*, 2003, **593**, 393–401.
2 K. Kawaguchi, E. Kagi, T. Hirano, S. Takano and S. Saito, *Astrophys. J.*, 1993, **406**, L39–L42.
3 L. M. Ziurys, A. J. Apponi, M. Guelin and J. Cernicharo, *Astrophys. J.*, 1995, **445**, L47–L50.
4 B. E. Turner, T. C. Steimle and L. Meerts, *Astrophys. J.*, 1994, **426**, L97–L100.
5 L. M. Ziurys, C. Savage, J. L. Highberger, A. J. Apponi, M. Guelin and J. Cernicharo, *Astrophys. J.*, 2002, **564**, L45–L48.
6 J. Cernicharo and M. Guelin, *Astron. Astrophys.*, 1987, **183**, L10–L12.
7 L. M. Ziurys, A. J. Apponi and T. G. Phillips, *Astrophys. J.*, 1994, **433**, 729–732.
8 A. Janczyk and L. M. Ziurys, *Astrophys. J.*, 2006, **639**, L107–L110.
9 S. T. Ridgway, D. F. Carbon and D. N. B. Hall, *Astrophys. J.*, 1978, **225**, 138–147.
10 S. T. Ridgway, D. N. B. Hall, S. G. Kleinmann, D. A. Weinberger and R. S. Wojslaw, *Nature*, 1976, **264**, 345–346.
11 I. Cherchneff and A. E. Glassgold, *Astrophys. J.*, 1993, **419**, L41–L44.
12 L. Manceron and L. Andrews, *J. Am. Chem. Soc.*, 1985, **107**, 563–568.
13 J. H. B. Chenier, J. A. Howard, B. Mile and R. Sutcliffe, *J. Am. Chem. Soc.*, 1983, **105**, 788–791.
14 P. H. Kasai, *J. Am. Chem. Soc.*, 1983, **105**, 6704–6710.
15 E. S. Kline, Z. H. Kafafi, R. H. Hauge and J. L. Margrave, *J. Am. Chem. Soc.*, 1985, **107**, 7559–7562.
16 J. R. Flores and A. Largo, *J. Phys. Chem.*, 1992, **96**, 3015–3021.
17 Y. M. Xie, B. F. Yates and H. F. Schaefer, *J. Am. Chem. Soc.*, 1990, **112**, 517–523.
18 J. S. Tse, *J. Am. Chem. Soc.*, 1990, **112**, 5060–5065.
19 G. V. Chertihin, L. Andrews and P. R. Taylor, *J. Am. Chem. Soc.*, 1994, **116**, 3513–3518.
20 D. W. Tokaryk, A. G. Adam and W. S. Hopkins, *J. Mol. Spectrosc.*, 2005, **230**, 54–61.
21 M. G. Li and J. A. Coxon, *J. Mol. Spectrosc.*, 1996, **176**, 206–210.
22 M. J. Dick, P. M. Sheridan, J. G. Wang and P. F. Bernath, *J. Mol. Spectrosc.*, 2005, **233**, 197–202.
23 H. Ding, T. W. Schmidt, T. Pino, A. E. Boguslavskiy, F. Guthe and J. P. Maier, *J. Chem. Phys.*, 2003, **119**, 814–819.
24 W. C. Wiley and I. H. McLaren, *Rev. Sci. Instrum.*, 1955, **26**, 1150–1157.
25 M. J. Frisch, G. W. Trucks, H. B. Schlegel, G. E. Scuseria, M. A. Robb, J. R. Cheeseman, V. G. Zakrzewski, J. A. Montgomery, Jr., R. E. Stratmann, J. C. Burant, S. Dapprich, J. M. Millam, A. D. Daniels, K. N. Kudin, M. C. Strain, O. Farkas, J. Tomasi, V. Barone, M. Cossi, R. Cammi, B. Mennucci, C. Pomelli, C. Adamo, S. Clifford, J. Ochterski, G. A. Petersson, P. Y. Ayala, Q. Cui, K. Morokuma, D. K. Malick, A. D. Rabuck, K. Raghavachari, J. B. Foresman, J. Cioslowski, J. V. Ortiz, A. G. Baboul, B. B. Stefanov, G. Liu, A. Liashenko, P. Piskorz, I. Komaromi, R. Gomperts, R. L. Martin, D. J. Fox, T. Keith, M. A. Al-Laham, C. Y. Peng, A. Nanayakkara, C. Gonzalez, M. Challacombe, P. M. W. Gill, B. G. Johnson, W. Chen, M. W. Wong, J. L. Andres, M. Head-Gordon, E. S. Replogle and J. A. Pople, *GAUSSIAN 98 (Revision A.7)*, Gaussian, Inc., Pittsburgh, PA, 1998.
26 R. E. Stratmann, G. E. Scuseria and M. J. Frisch, *J. Chem. Phys.*, 1998, **109**, 8218–8224.
27 C. W. Western, PGOPHER, a Program for Simulating Rotational Structure, University of Bristol, Bristol, UK, http://pgopher.chm.bris.ac.uk.
28 I. Gerasimov, X. Yang and P. J. Dagdigian, *J. Chem. Phys.*, 1999, **110**, 220–228.
29 P. Jenniskens and F. X. Desert, *Astron. Astrophys., Suppl. Ser.*, 1994, **106**, 39–78.

Electronic Spectrum of the AlC_2 Radical

Egor Chasovskikh, Evan B. Jochnowitz, Eunsook Kim, and John P. Maier*

Department of Chemistry, University of Basel, Klingelbergstrasse 80, CH-4056 Basel, Switzerland

Isabelle Navizet

Université Paris-Est, Laboratoire de Chimie Théorique, 5 bd Descartes, F-77454 Marne la Vallée cedex 2, France

Received: July 3, 2007; In Final Form: September 5, 2007

An electronic transition of the AlC_2 radical (C_{2v} structure) has been observed using laser-induced fluorescence spectroscopy. The molecule was prepared in a supersonic expansion by ablation of an aluminum rod in the presence of acetylene gas. A spectrum was recorded in the 451−453 nm region and assigned to the $\tilde{C}\,^2B_2-\tilde{X}\,^2A_1$ system (T_0 = 22102.7 cm^{-1}) based on a rotational analysis and agreement with calculated molecular parameters and excitation energies. Ab initio results obtained using couple cluster methods are in accord with previous theoretical work which concludes that ground-state AlC_2 possesses a T-shaped C_{2v} $^2A_1$ geometry, with the linear $^2\Sigma^+$ AlCC isomer 0.70 eV higher in energy. A fit of the experimental spectrum yields rotational constants in the ground and electronically excited states that are in reasonable agreement with the calculated values: A'' = 1.7093(107), B'' = 0.4052(50), C'' = 0.3228(49) cm^{-1} for the $\tilde{X}\,^2A_1$ state, and A' = 1.5621(137), B' = 0.4028(46), C' = 0.3201(54) cm^{-1} for $\tilde{C}\,^2B_2$. Variation in individual fluorescence lifetimes suggests that the emitting $\tilde{C}\,^2B_2$ state undergoes rovibronic mixing with lower lying electronic states.

Introduction

Metal carbides play an important role in the field of catalytic reactions, mainly due to the large surface areas that they tend to possess. Other recent advances in coating technologies have further fueled research in these compounds. Interest in gas-phase studies stems from the fact that smaller metal carbides are predicted to exist in space. While carbon is the most abundant heavy element in interstellar space, aluminum compounds containing halides, such as AlCl and AlF, as well as AlNC, have been detected in the inner circumstellar envelopes of carbon-rich stars through their rotational transitions.[1,2]

Dicarbides became a curiosity when both experiments and theory demonstrated that SiC_2 possesses a T-shaped geometry,[3,4] which was in direct conflict with the linear ground state structure of C_3.[5,6] Among theorists, there is general agreement that AlC_2 also has a T-shaped structure, with the C_{2v} conformation 33.5−46 kJ mol^{-1} more stable than the linear $C_{\infty v}$ geometry.[7−11] The high electron affinity of C_2 also suggests that stable dicarbides are likely formed with electropositive metals possessing low-ionization potentials, such as Al, Mg, or B.[12] Similarly, vibrational, rotational, and hyperfine structure in high-resolution spectra for the $\tilde{A}\,^2A_1$ - $\tilde{X}\,^2A_1$ transition of T-shaped YC_2 have also been analyzed.[13,14] Optical Stark measurements on the origin band led to the determination of a large dipole moment (6.38 D in the $\tilde{X}\,^2A_1$ state) confirming that the bonding in YC_2 is highly ionic.[15] Any structural parameters obtained from studying AlC_2 will help expand the understanding of more complex metal carbide systems. Spectroscopically determined constants offer a means to identify these molecules in interstellar environments.

Recent structural calculations found that the C_{2v} T-shaped structure is more stable than the linear $C_{\infty v}$ geometry by 47.66 kJ mol^{-1} using a single point QCISD(T) calculation (36.69 kJ mol^{-1} using DFT B3LYP).[10] The same study reports a 37.20 kJ mol^{-1} barrier (B3LYP) for isomerization from the T-shape to linear form, versus a 0.50 kJ mol^{-1} barrier for the reverse reaction, thus indicating that any linear $C_{\infty v}$ AlC_2 will be easily converted into the C_{2v} isomer.

Previous experimental work on the AlC_2 radical includes electron spin resonance studies in rare gas matrices.[16] Here, the T-shaped structure of AlC_2 was confirmed and led to the assignment of the $\tilde{X}\,^2A_1$ ground state. Bonding characteristics were also analyzed, indicating that the aluminum atom interacts with C_2 by donating electron density to the more electronegative C_2 through both $\sigma-$ and π-molecular orbitals.

Although AlC_2 has not yet been detected in the IR, theoretical methods have been used to calculate vibrational frequencies in the ground state: a single point QCISD optimization yielded the low-frequency b_2 mode (404.8 cm^{-1}) and the two a_1 vibrational modes (624.4 and 1761 cm^{-1}).[10] CASSCF theory with a VDZ basis set reports frequencies of 442, 680.2, and 1733.1 cm^{-1} for the same vibrations.[8]

The energy difference between the $\tilde{X}\,^2A_1$ and $\tilde{A}\,^2A_1$ states in neutral AlC_2 was determined as 0.98 eV through an analysis of the photoelectron spectrum of the AlC_2^- anion.[17] A vibrational progression was assigned to a 590 cm^{-1} Al−C_2 stretch in both the ground and excited $^2A_1$ states.

Rotational constants for the equilibrium structures of the T-shaped AlC_2 radical were calculated as: A_e = 50.76, B_e = 12.00, and C_e = 9.705 GHz.[7] A more recent study, using a B3LYP/6-311G(d) method, reports A_e = 52.657, B_e = 11.814, and C_e = 9.650 GHz for a similar T-shaped structure.[11]

Experimental Section

Jet-cooled AlC_2 was produced using laser vaporization (532 nm) of a pure aluminum rod in the flow of 5% acetylene in

* Corresponding author. E-mail: j.p.maier@unibas.ch. Phone: +41 61 267 38 26. Fax: +41 61 267 38 55.

10.1021/jp075169e CCC: $37.00
Published on Web 10/30/2007 PAGE EST: 3.7

TABLE 1: Optimized Geometry for $\tilde{X}\,^2A_1$ (C_{2v}) AlC_2 and Calculated Vibrational Frequencies (cm^{-1})

	CCSD(T)	QCISD/6-311G* (ref 10)
r_{C-C}	1.276 Å	1.280 Å
r_{Al-C}	1.928 Å	1.937 Å
α_{C-Al-C}	38.7°	38.6°
ω_1 a_1	1735	1761
ω_2 a_1	645	624
ω_3 b_2	421	405

TABLE 2: Vertical Transition Energies (eV) for Excitations with Transition Moments Greater than 0.2 a.u., Calculated at the Minimum Geometry

transition	CASSCF	MRCI+Q	transition moment (a.u.)
$\tilde{A}\,^2A_1 - \tilde{X}\,^2A_1$	1.195	1.200	0.995 (*Z*)
$\tilde{F}\,^2A_1 - \tilde{A}\,^2A_1$	3.011		−0.470 (*Z*)
$\tilde{E}\,^2B_2 - \tilde{C}\,^2B_2$	0.809		0.394 (*Z*)
$\tilde{B}\,^2B_1 - \tilde{A}\,^2A_1$	1.024		−0.334 (*X*)
$\tilde{D}\,^2B_1 - \tilde{X}\,^2A_1$	2.947	3.271	0.335 (*X*)
$\tilde{D}\,^2B_1 - \tilde{A}\,^2A_1$	1.752		−0.230 (*X*)
$\tilde{C}\,^2B_2 - \tilde{X}\,^2A_1$	2.770	2.752	0.471 (*Y*)
$\tilde{E}\,^2B_2 - \tilde{X}\,^2A_1$	3.580	3.830	0.422 (*Y*)
$\tilde{E}\,^2B_2 - \tilde{A}\,^2A_1$	2.385		0.367 (*Y*)

helium or argon gas (10 bar) provided by a 0.3 mm orifice-pulsed valve. The rod was rotated and translated so that a fresh surface was continuously exposed to the laser, which was fired to coincide with the gas flow over the target area. The vaporization plume flows through a channel (3 mm diameter by 5 mm long) before undergoing a free-jet expansion.

The resulting AlC_2 radicals are then probed through laser-induced fluorescence (LIF) using an excimer-pumped dye laser (0.15 cm^{-1}) with a wavemeter used for frequency calibration. The fluorescence signal was collected by an *f*/1 lens and detected using a photomultiplier and a digital oscilloscope.

Results

Ab initio calculations using the MOLPRO program[18] with an aug-cc-pVQZ basis set of Dunning et al.[19,20] were carried out for the electronic states of AlC_2. The coupled cluster with perturbative triples (CCSD(T)) method was used for the description of the $\tilde{X}\,^2A_1$ ground state. For comparison, the ground-state linear $^2\Sigma_g^+$ isomer AlCC was also calculated and found to lie 0.70 eV higher in energy. The optimized geometries for the electronic C_{2v} ground state and the harmonic frequencies of the fundamental vibrational transitions are compared with previous work in Table 1.[10]

The vertical transition energies for the lowest excited states whose transition moments are greater than 0.2 au are listed in Table 2 at the ground state equilibrium geometry. Full valence CASSCF calculations were performed with 8 states (3 a_1, 2 b_1, 2 b_2, 1 a_2, all in C_{2v} symmetry). Higher level calculations for vertical transitions originating from the $\tilde{X}\,^2A_1$ state have also been performed at the MRCI level of theory with the results listed in Table 2. Finally, the excited $\tilde{C}\,^2B_2$ state has been optimized at the MRCI level of theory in C_{2v} geometry. The minimum lies 2.684 eV above the $\tilde{X}\,^2A_1$ ground state. The geometries calculated for the upper and lower states are shown in Figure 1.

The bottom trace in Figure 2 shows the experimental spectrum (0.15 cm^{-1} resolution) for the $\tilde{C}\,^2B_2 - \tilde{X}\,^2A_1$ transition of AlC_2. The signal was dependent on the presence of aluminum. The spectrum was not observed when acetylene was missing from the buffer gas mixture, indicating that carbon and/or hydrogen must be present in the spectral carrier. Substituting deuterated acetylene had no effect, thus eliminating the role of hydrogen.

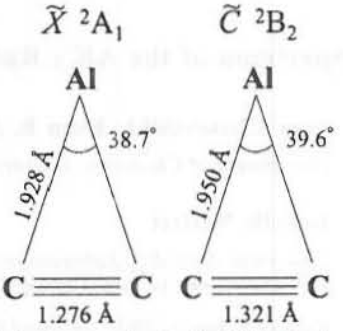

Figure 1. Optimized geometries for the AlC_2 radical calculated at the CASSCF level of theory.

The recorded spectrum was thus assigned to the $\tilde{C}\,^2B_2 - \tilde{X}\,^2A_1$ transition of AlC_2, one of the stronger transitions listed in Table 2, based on its observed frequency. Scanning to the red revealed no additional band systems, thereby allowing a confident assignment of the observed band as the origin of the $\tilde{C}\,^2B_2 - \tilde{X}\,^2A_1$ transition.

Decay curves were measured for 21 rotational peaks in the origin band of the $\tilde{C}\,^2B_2 - \tilde{X}\,^2A_1$ transition of AlC_2, in the range from 22 065 to 22 116 cm^{-1}. The decay curves appeared exponential and were found to vary from 140 to 640 ns. This substantial scatter is shown graphically in Figure 3 where the measured lifetimes are plotted above a portion of the experimental spectrum reproduced from Figure 2.

Discussion

A rotational analysis using the program "WANG" was performed with a conventional Hamiltonian for an asymmetric top assuming a *b*-type transition in a C_{2v} molecule.[21] In particular six Q-branch heads, which are associated with $\Delta K \pm 1$ sub-bands that result from the perpendicular nature of the transition, were used to guide the fit. These are labeled in Figure 2 using the notation $Q(K_a' - K_a'')$. In all, a selection of 14 lines, including P-branch lines from the $K_a' - K_a''$ (3−4) and $K_a' - K_a''$ (1−0) manifolds, was included in the least-squares optimization to obtain the best parameters for the rotational analysis. Any increase in the number of fitted lines tended to be detrimental to achieving a successful fit, presumably because of the substantial blending of lines due to the limited resolution achievable in measuring the experimental spectrum. The temperature used for modeling the spectrum was 70 K and the line width was fixed at 0.15 cm^{-1}. The resulting simulation is shown as the upper trace in Figure 2.

As with SiC_2,[3] the two carbon atoms in this molecule are equivalent and interchangeable through rotation around the "*a*"-inertial axis. In a near-prolate asymmetric top, equivalent zero spin nuclei that are symmetric with respect to rotation about the "*b*"-axis will produce alternation in the *J* structure. Here, in a C_{2v} geometry, the equivalent zero-spin nuclei are identical through 2-fold rotation about the *a*-axis, producing alternation in the *K* rotational structure (K_a). For AlC_2 the nuclear spin statistical weights of odd K_a'' levels ($K_a'' = 1, 3, \ldots$) are zero, hence there should be no evidence of any sub-bands originating from these states. Taking into account these alternation effects is essential for the fitted spectrum to more closely resemble the observed one, offering further verification of the spectral carrier.

However, as may be seen from the comparison shown in Figure 2, a perfect fit between the rotational analysis and the experimental spectrum was not achieved. This may be attributed to two factors. One possibility is that $\tilde{C}\,^2B_2$ rovibronic levels

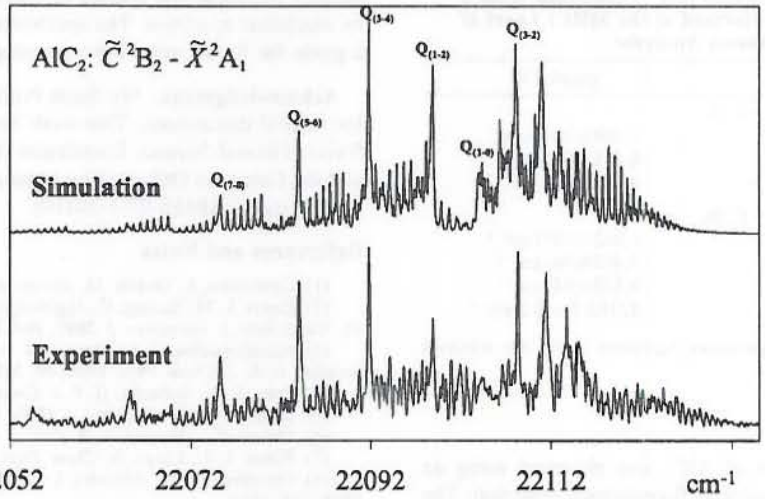

Figure 2. The origin band in the $\tilde{C}\,^2B_2 - \tilde{X}\,^2A_1$ electronic transition for AlC_2, recorded via laser-induced fluorescence. The lower trace is the experimental spectrum, while the upper trace depicts the simulated fit. Q-branch heads that are associated with $\Delta K \pm 1$ sub-bands and were used to guide the spectral fit are labeled $Q(K_a' - K_a'')$.

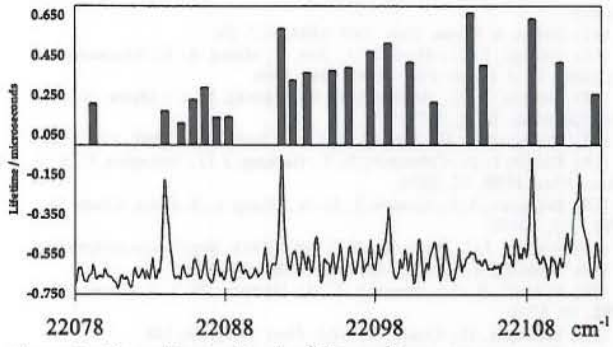

Figure 3. The origin band in the $\tilde{C}\,^2B_2 - \tilde{X}\,^2A_1$ electronic transition for AlC_2, reproduced from Figure 2. Above the spectrum lie depictions of the fluorescent lifetimes measured.

are perturbed as a result of rovibronic coupling with levels associated with lower lying electronic states. These can include near-degenerate b_2 levels of the $\tilde{A}\,^2A_1$ and $\tilde{X}\,^2A_1$ states or lower lying quartet states that have not yet been located. Through vibronic and Coriolis operators A_1, A_2, and B_1 states may also interact in a rotational-dependent manner, thus perhaps also perturbing the observed system.

The lifetimes of various lines in the spectrum were measured in an effort to qualitatively examine the extent of mixing among the electronic states in AlC_2, giving rise to the wide variation in τ depicted in Figure 3. In an earlier study on the $\tilde{A}\,^1B_1 - \tilde{X}\,^1A_1$ transition of SiH_2 (C_{2v}), wide variations in the fluorescent lifetimes of individual rotational lines (few nanoseconds to >1 μs) were attributed to rovibronic perturbations.[22,23] Specifically, rovibronic levels in the SiH_2 $\tilde{A}\,^1B_1$ state mix with background levels from either the lower lying $\tilde{a}\,^3B_1$ state or highly excited vibrational levels from the $\tilde{X}\,^1A_1$ ground state, leading to perturbations in the energy levels and oscillator strengths and thus making a spectral fit impossible using a standard rotational Hamiltonian. Similar behavior has also been reported for the fluorescence decay rates found in the S_1 ($\tilde{A}^1A_2$) states of formaldehyde.[24,25]

This mixing can be sensitive to rotational quantum number[26] and the proximity and identity of near degenerate background states, leading to seemingly random perturbations in oscillator strengths and energy level positions and thereby influencing the experimental measurement of the rotational contour. Figure 3 shows that some Q-branch band maxima associated with the $\Delta K \pm 1$ sub-bands possess lifetimes up to 2−3 times longer than other lines. These longer lifetimes may arise due to quartet dilution, whereby a substantial fraction of spin forbidden quartet character is added to the emitting $\tilde{C}\,^2B_2$ state. Conversely, other high J-levels demonstrate shortened lifetimes, which may be due to a stronger coupling with b_2 vibronic states from the $\tilde{A}\,^2A_1$ and $\tilde{X}\,^2A_1$ electronic states, resulting in increased non-radiative decay rates.

A second reason for the imperfect fit to the experimentally observed spectrum may derive from a non-Boltzmann temperature distribution in the jet: that is, in an expanding jet the J-levels cool more efficiently than the K-levels. This has been previously observed in beams of glyoxal[27] and acetaldehyde[28] that were also studied using LIF. In the case of acetaldehyde, the rotational temperature for molecules in the beam was found to be over four times higher in K-quantum number than in J. This same effect is apparent in the spectral simulation of AlC_2, where at 70 K the J-temperature seems to fit reasonably well; however, the intensity distribution in the Q-branch heads appears to fall faster than in the experimental spectrum. This would seem to indicate that to correctly simulate the spectrum one would have to model an increased K-temperature while holding the J-temperature at its current value. This has not been carried out at this stage because a reasonable fit was obtained yielding rotational constants consistent with the theoretical structures calculated for the $\tilde{X}\,^2A_1$ and $\tilde{C}\,^2B_2$ states.

The molecular constants obtained are given in Table 3, along with the corresponding MRCI calculated values. Conservative errors were qualitatively estimated through fixing the resulting constants and then systematically varying each parameter. In general, constants could be varied by approximately twice the value of the standard deviations derived from the spectral fitting procedure before the modeled spectrum significantly differed from the experimentally obtained one. Error in T_0 stems from the spectral line width used to measure the transition.

Geometric structures can be estimated from the rotational constants derived in the spectroscopic fit, with the C−C bond length calculated directly from the A constants. This yields r_{Al-C} and r_{C-C} as 1.93 and 1.28 Å for the $\tilde{X}\,^2A_1$ ground state, and 1.94 and 1.34 Å for the excited $\tilde{C}\,^2B_2$ state. All values are within error of the calculated CASSCF geometries shown in Figure 1.

TABLE 3: Rotational Constants (cm^{-1}) Obtained from a Geometry Optimization Performed at the MRCI Level of Theory and from the Rotational Analysis[a]

	MRCI	spectral fit
	$\tilde{X}\,^2A_1$	
A″	1.725 cm^{-1}	1.7093(107) cm^{-1}
B″	0.400 cm^{-1}	0.4052(50) cm^{-1}
C″	0.325 cm^{-1}	0.3228(49) cm^{-1}
	$\tilde{C}\,^2B_2$	
A′	1.609 cm^{-1}	1.5621(137) cm^{-1}
B′	0.394 cm^{-1}	0.4028(46) cm^{-1}
C′	0.316 cm^{-1}	0.3201(54) cm^{-1}
T_0		22102.7 ± 0.2 cm^{-1}

[a] Errors in the rotational constants represent twice the standard deviations derived from the fit.

Conclusion

The electronic spectrum of AlC_2 was observed using an ablation source and laser induced fluorescence detection. The experiments demonstrated that the spectral carrier contained only Al and C atoms. The rotationally resolved spectrum was assigned to the origin band of the $\tilde{C}\,^2B_2-\tilde{X}\,^2A_1$ system, a species that exists in a planar C_{2v} geometry as previously calculated. A rotational analysis is consistent with the asymmetric top AlC_2 (C_{2v}), further evidenced by the fact that nuclear spin effects due to two equivalent carbon atoms must be considered to properly model the experimental spectrum.

Molecular constants were estimated using a spectral simulation based on a least-squares fit to 14 individual lines. Spectroscopic constants obtained from the fit compare reasonably well with ab inito calculations performed on both the ground and excited states. The imperfect nature of the fit is attributed to an inability to account for substantial interactions with lower lying quartet and $^2A_1$ states that manifest themselves as irregular perturbations in both the energy levels and their oscillator strengths. Being able to incorporate a non-Boltzmann temperature dependence for the *J*- and *K*-levels may also enable a more accurate fit. However, as it stands, the fit confirms the perpendicular nature of the $\tilde{C}\,^2B_2-\tilde{X}\,^2A_1$ transition.

Finally, further confirmation of the carrier's identity was obtained using a resonant 2-color 2-photon ionization technique, where a spectrum of AlC_2 was observed in the same 452 nm region for the *m/z* 51 mass.[29] A more detailed analysis awaits the collection of a higher resolution spectrum.

No matches corresponding to the diffuse interstellar band literature were found for the origin band of AlC_2; however, the information obtained in this study can aid further attempts to identify this dicarbide species in interstellar space by means of its electronic spectrum. The spectroscopic constants also offer a guide for future microwave investigations.

Acknowledgment. We thank Professor Alan E. W. Knight for helpful discussions. This work has been supported by the Swiss National Science Foundation (Grant 200020-115864/1) and the European Office of Aerospace Research and Development (Grant FA8655-07-1-30310).

References and Notes

(1) Cernicharo, J.; Guélin, M. *Astron. Astrophys.* **1987**, *183*, L10.
(2) Ziurys, L. M.; Savage, C.; Highberger, J. L.; Apponi, A. J.; Guélin, M.; Cernicharo, J. *Astrophys. J.* **2002**, *564*, L45.
(3) Michalopoulos, D. L.; Geusic, M. E.; Langridge-Smith, P. R. R.; Smalley, R. E. *J. Chem. Phys.* **1984**, *80*, 3556.
(4) Grev, R. S.; Schaefer, H. F. *J. Chem. Phys.* **1984**, *80*, 3552.
(5) Douglas, A. E. *Astrophys. J.* **1951**, *114*, 466.
(6) Clusius, K.; Douglas, A. E. *Can. J. Phys.* **1954**, *32*, 319.
(7) Flores, J. R.; Largo, A. *Chem. Phys.* **1990**, *140*, 19.
(8) Chertihin, G. V.; Andrews, L.; Taylor, P. R. *J. Am. Chem. Soc.* **1994**, *116*, 3513.
(9) Yang, H.; Tanaka, K.; Shinada, M. *THEOCHEM-J. Mol. Struct.* **1998**, *422*, 159.
(10) Zheng, X.; Wang, Z.; Tang, A. *J. Phys. Chem. A* **1999**, *103*, 9275.
(11) Redondo, P.; Barrientos, C.; Largo, A. *Int. J. Quantum Chem.* **2004**, *96*, 615.
(12) Green, S. *Chem. Phys. Lett.* **1984**, *112*, 29.
(13) Steimle, T. C.; Marr, A. J.; Xin, J.; Merer, A. J.; Athanassenas, K.; Gillet, D. *J. Chem. Phys.* **1997**, *106*, 2060.
(14) Steimle, T. C.; Bousquet, R. R.; Namiki, K. C.; Merer, A. J. *J. Mol. Spectrosc.* **2002**, *215*, 10.
(15) Bousquet, R. R.; Steimle, T. C. *J. Chem. Phys.* **2001**, *114*, 1306.
(16) Knight, L. B.; Cobranchi, S. T.; Herlong, J. O.; Arrington, C. A. *J. Chem. Phys.* **1990**, *92*, 5856.
(17) Boldyrev, A. I.; Simons, J.; Li, X.; Wang, L.-S. *J. Am. Chem. Soc.* **1999**, *121*, 10193.
(18) Werner, J.-J.; Knowles, P. J. MOLPRO; http://www.molpro.net.
(19) Dunning, T. H. *J. Chem. Phys.* **1989**, *90*, 1007.
(20) Kendall, R. A.; Dunning, T. H.; Harrison, R. J. *J. Chem. Phys.* **1992**, *96*, 6796.
(21) Luckhaus, D.; Quack, M. *Mol. Phys.* **1989**, *68*, 745.
(22) Thoman, J. W.; Steinfeld, J. I.; McKay, R. I.; Knight, A. E. W. *J. Chem. Phys.* **1987**, *86*, 5909.
(23) McKay, R. I.; Uichanco, A. S.; Bradley, A. J.; Holdsworth, J. R.; Francisco, J. S.; Steinfeld, J. I.; Knight, A. E. W. *J. Chem. Phys.* **1991**, *95*, 1688.
(24) Weisshaar, J. C.; Moore, C. B. *J. Chem. Phys.* **1980**, *72*, 5415.
(25) Guyer, D. R.; Polik, W. F.; Moore, C. B. *J. Chem. Phys.* **1986**, *84*, 6519.
(26) Knight, A. E. W. Rotational Involvement in Intramolecular Vibrational Redistribution. In *Excited States*; Lim, E. C., Ed.; Academic Press: New York, 1988; Vol. 7.
(27) Peyroula, E. P.; Jost, R. *J. Mol. Spectrosc.* **1987**, *121*, 167.
(28) Price, J. M.; Mack, J. A.; von Helden, G.; Yang, X.; Wodtke, A. M. *J. Phys. Chem.* **1994**, *98*, 1791.
(29) Apetrei, C.; Chasovskikh, E.; Ding, H.; Jochnowitz, E. B.; Maier, J. P. In preparation.